JOURNAL OF THE KOREAN ASTRONOMICAL SOCIETY
33: 143~149, 2000

# PHOTOMETRIC STUDY OF THE OLD OPEN CLUSTER TOMBAUGH 2

JAE-MANN KYEONG[1] AND YONG-IK BYUN[2]

[1]Korea Astronomy Observatory, Taejon 305-348, Korea
*E-mail: jman@kao.re.kr*
[2]Department of Astronomy, Yonsei University, Seoul 120-749, Korea
*E-mail: byun@darksky.yonsei.ac.kr*
*(Received Dec. 5, 2000; Accepted Dec. 11, 2000)*

## ABSTRACT

We present the results of near-IR band (*JHK*) photometric study for the old open cluster To 2. Combined with existing optical data, our IR photometry is used to derive the reddening $E(B-V)=0.24\pm0.12$ and the distance $(m-M)_0=14.6\pm0.42$. Comparison with theoretical isochrones suggests the age and metallicity of To 2 are log $t\sim9.3$ and [Fe/H]$\sim-0.3$, respectively.

*Key words*: infrared photometry, open cluster, To 2

## I. INTRODUCTION

Open clusters have been regarded as important tools in the study of the early evolution of Galactic disk because their formation epoch can be dated relatively easily and they can be seen to large distances.

The distant open cluster Tombaugh 2($\alpha(1950)=7^h$ $01^m$, $\delta(1950)=-20°47'$, hereafter referred as To 2) is located in the outer Galactic disk. To 2 is therefore important in the investigation the age-metallicity relation and radial abundance gradient across the disk of our Galaxy (Friel 1995). However, the distance, age and metallicity information for this cluster have been rather conflicting to each other. Adler & Janes (1982) determined $E(B-V)=0.07$ and $(m-M)_V=15.6$ from photographic observation. Geisler (1987) measured a mean metallicity of [Fe/H]$=-1.2$ from Washington photoelectric photometry of some of To 2 giant stars. More recently Friel & Janes (1993) made the extensive spectroscopic observation of the giant stars to confine the disk radial gradient and age-metallicity relationships in the Galaxy, and derived [Fe/H]$=-0.60$ with $E(B-V)=0.20$. But they observed only two stars in To 2 to derive its metallicity and their later spectroscopic observation using CTIO and KPNO 4m telescopes and multi-object spectrographs gave the metallicity of To 2 as $-0.35$ (Friel et al., 1995). On the other hand, Kubiak et al. (1992) obtained deep photometric($V\sim21$) data on To 2. According to them, the distance to the cluster is 6.3 kpc and $E(B-V)=0.40$. Although there have been many observations both photometric and spectroscopic, the important basic parameters have remained largely uncertain, that is, reddening 0.1~0.4, [Fe/H]$=-0.3\sim-1.2$, age 1.7~4 Gyr, and distance 6~13 kpc. In this paper, we present a study of To 2 based on optical and near-infrared *JHK* band data. This is the first extensive near-infrared photometry for this cluster. Based on theoretical isochrone analysis, we have also estimated the basic parameters of this cluster, reddening, distance modulus, metallicity and age. In Section II, we describe our near-IR observation and data reduction. Section III present the photometry, calibration and resulting Color-Magnitude Diagram (CMD) of the IR band. In Section IV, we derive reddening, distance modulus, age, and metallicity using the fitting of isochrone with Kubiak et al. (1992) *BV* CCD data. Section V summarizes our results.

## II. OBSERVATION AND DATA REDUCTION

*JHK* images of old open cluster To 2 were obtained over the night in UT 1996 December 23 using the 2.3 m telescope and the IR camera CASPIR at the Siding Spring Observatory. This observation was a part of our general near-infrared study for galactic clusters. CASPIR gives gain=9$e^-$ per ADU and readout noise as 50 electrons. The detector of CASPIR was InSb chip of 256 ×256 format and the image scale was 0".50/pixel, which gave the sky coverage of 2.1×2.1 arcmin$^2$. Since the field of view is very small, we did 2×2 mosaic observation to cover the wide field of To 2. Each data frame was obtained with 1 second exposure time and 20 cycles, which means that each image is a result of combining 20 frames of the same exposure. The mean seeing of the night was ~2".0 FWHM. Throughout the

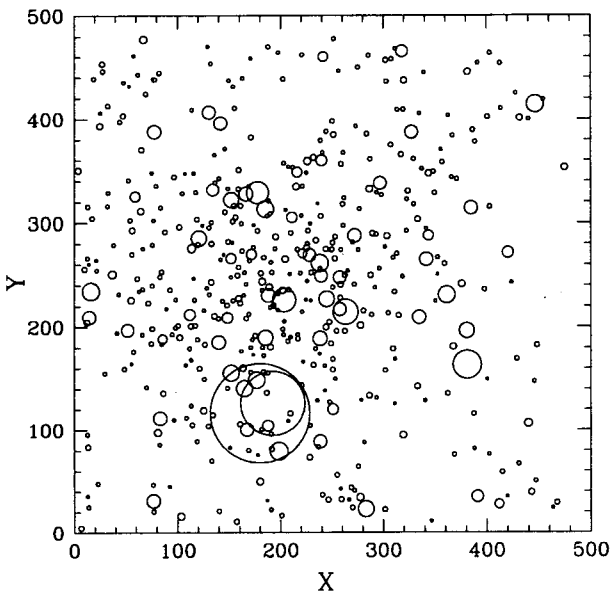


**Fig. 1.** Synthetic map (4'×4') of To 2 as observed in the $K$ band. North is top, east left. The brightest star is $K\sim8$. The two brightest stars are probably field stars. The plate scale is 0".50/pixel.

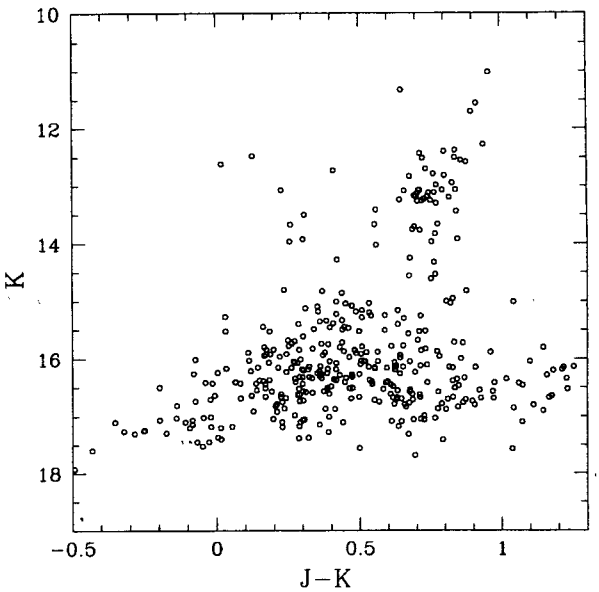


**Fig. 2.** The near-infrared CMD of To 2.

night, we frequently obtained bias frames because the bias level was known to vary at the time of observations. The observed field (4'×4') is shown in Fig. 1. In the figure, each star is represented by an open circle whose size is proportional to the brightness.

In order to transform instrumental magnitudes to the standard system, we observed several IRIS photometric standard stars (McGregor 1995) throughout ourblankobserving run of 6 nights.

The IR data reduction method is more complex than optical CCD data, because of high sky background and its rapid variability. The CASPIR detector array also shows a quadratic non-linearity, which should be linearized to recover the low and high intensity information accurately (McGregor 1995). Each data frame was bias and dark subtracted and, a set of processed data frames from a mosaic sequence were then median-combined to create a sky frame for that sequence. After subtracting corresponding sky frames, the data images were subjected to flatfielding. We used flatfields obtained by turning on and off the dome light in the beginning and end of each observing nights. Several such exposures were performed in each filter in order to achieve good signal statistics for dome flats.

## III. PHOTOMETRY, CALIBRATION AND C-M DIAGRAM

Stellar photometry was performed using the point spread function fitting package of DAOPHOT and ALLSTAR, as well as DAOMATCH and DAOMASTER routines to identify and match stars in different data frames (Stetson 1992).

Instrumental magnitude were transformed using standardization formulae we derived from the aperture photometry of standard stars. The transformation formulae are as follows.

$$m_J=4.819+J+0.112\ X_J-0.113(J-K)$$
$$m_H=4.891+H+0.095X_H-0.056(J-H)$$
$$m_K=5.700+K+0.118X_K$$

where lower case represents instrumental magnitude, and upper case standard magnitude. $X$ refers to airmass. In case of $K$ band, the coefficient of color term is so insignificant that we neglected the term. In calculating airmass coefficients and coefficients of color term we used 6 nights standard star data, with particular attention to night-to-night zero point variation of about 0.2 magnitude. The RMS differences between our observations and the standard system are 0.017, 0.020, 0.022 mag in $J$, $H$ and $K$, respectively. Table 1 lists the photometry of the bright star($K$<16 mag) of To 2. The $X$ and $Y$ coordinates listed in Table 1 are given in units of the pixel(=0".50).

The resulting CMD of our IR photometry is shown in Fig. 2. No evident main sequence turnoff can be seen in our IR CMD, although there is a turnoff point near $V$ ~18.1, $(B-V)\sim0.8$ in Kubiak et al. (1992)'s optical data. The uncertainty of near-infrared data increases rapidly below $K\sim16$ making the turnoff difficult to recognize. Later analysis is therefore based on those stars that appear both in optical and in our near-infrared observations. The mean magnitude and color of red giant clump star in IR CMD is located at $K=13.18$, $J-K=0.73$.

## IV. BASIC PARAMETERS OF TO 2

Kubiak et al. (1992) observed this cluster in $BVI_c$

**Table 1.** Observed JHK data of To 2

| ID | X | Y | $J$ | $\sigma_J$ | $H$ | $\sigma_H$ | $K$ | $\sigma_K$ |
|---|---|---|---|---|---|---|---|---|
| 1 | 180.21 | 116.26 | 8.79 | 0.01 | 7.57 | 0.03 | 7.43 | 0.03 |
| 2 | 192.49 | 125.88 | 9.94 | 0.02 | 8.86 | 0.01 | 8.67 | 0.02 |
| 3 | 381.11 | 163.43 | 11.97 | 0.02 | 11.11 | 0.01 | 11.02 | 0.02 |
| 4 | 263.61 | 214.38 | 11.98 | 0.02 | 11.38 | 0.02 | 11.33 | 0.03 |
| 5 | 203.66 | 225.78 | 12.47 | 0.01 | 11.63 | 0.02 | 11.56 | 0.02 |
| 6 | 177.68 | 328.99 | 12.60 | 0.02 | 11.80 | 0.02 | 11.70 | 0.03 |
| 7 | 361.39 | 230.91 | 12.60 | 0.02 | 12.46 | 0.02 | 12.48 | 0.03 |
| 8 | 283.15 | 23.01 | 12.64 | 0.02 | 12.57 | 0.02 | 12.62 | 0.03 |
| 9 | 198.63 | 79.29 | 13.21 | 0.02 | 12.36 | 0.02 | 12.27 | 0.03 |
| 10 | 238.33 | 261.45 | 13.21 | 0.03 | 12.44 | 0.02 | 12.37 | 0.05 |
| 11 | 446.58 | 414.33 | 13.14 | 0.02 | 12.47 | 0.02 | 12.43 | 0.04 |
| 12 | 16.11 | 234.45 | 13.19 | 0.03 | 12.49 | 0.03 | 12.39 | 0.04 |
| 13 | 176.90 | 148.70 | 13.24 | 0.02 | 12.59 | 0.01 | 12.51 | 0.03 |
| 14 | 185.35 | 313.18 | 13.34 | 0.02 | 12.57 | 0.02 | 12.50 | 0.03 |
| 15 | 165.06 | 140.38 | 13.41 | 0.02 | 12.61 | 0.01 | 12.55 | 0.02 |
| 16 | 152.12 | 155.52 | 13.46 | 0.02 | 12.66 | 0.01 | 12.58 | 0.03 |
| 17 | 120.96 | 285.29 | 13.14 | 0.02 | 12.76 | 0.01 | 12.73 | 0.02 |
| 18 | 245.14 | 226.88 | 13.44 | 0.02 | 12.74 | 0.02 | 12.70 | 0.05 |
| 19 | 380.71 | 196.37 | 13.55 | 0.03 | 12.85 | 0.01 | 12.79 | 0.03 |
| 20 | 185.57 | 189.74 | 13.51 | 0.02 | 12.87 | 0.02 | 12.83 | 0.03 |
| 21 | 152.11 | 322.01 | 13.62 | 0.02 | 12.88 | 0.01 | 12.82 | 0.02 |
| 22 | 83.39 | 111.49 | 13.30 | 0.02 | 13.05 | 0.02 | 13.07 | 0.03 |
| 23 | 238.67 | 188.97 | 13.77 | 0.02 | 13.02 | 0.02 | 12.94 | 0.03 |
| 24 | 166.36 | 327.65 | 13.76 | 0.03 | 13.06 | 0.02 | 12.98 | 0.02 |
| 25 | 272.23 | 287.75 | 13.79 | 0.02 | 13.11 | 0.02 | 13.08 | 0.05 |
| 26 | 334.91 | 209.36 | 13.74 | 0.03 | 13.14 | 0.02 | 13.08 | 0.03 |
| 27 | 140.14 | 185.29 | 13.78 | 0.02 | 13.12 | 0.02 | 13.07 | 0.03 |
| 28 | 76.87 | 30.84 | 13.86 | 0.02 | 13.12 | 0.02 | 13.07 | 0.03 |
| 29 | 14.62 | 209.41 | 13.84 | 0.02 | 13.15 | 0.02 | 13.13 | 0.04 |
| 30 | 188.14 | 230.38 | 13.91 | 0.02 | 13.14 | 0.02 | 13.06 | 0.03 |
| 31 | 341.79 | 265.07 | 13.87 | 0.03 | 13.17 | 0.02 | 13.12 | 0.05 |
| 32 | 77.50 | 387.74 | 13.88 | 0.03 | 13.19 | 0.02 | 13.11 | 0.04 |
| 33 | 238.82 | 88.82 | 13.87 | 0.02 | 13.21 | 0.02 | 13.17 | 0.03 |
| 34 | 384.84 | 314.24 | 13.89 | 0.03 | 13.21 | 0.02 | 13.19 | 0.04 |
| 35 | 258.17 | 216.92 | 13.89 | 0.03 | 13.22 | 0.02 | 13.24 | 0.04 |
| 36 | 130.37 | 406.52 | 13.92 | 0.03 | 13.24 | 0.02 | 13.18 | 0.05 |
| 37 | 141.51 | 395.91 | 13.93 | 0.03 | 13.25 | 0.02 | 13.19 | 0.02 |
| 38 | 167.46 | 100.37 | 14.02 | 0.03 | 13.26 | 0.02 | 13.20 | 0.04 |
| 39 | 327.33 | 387.22 | 13.96 | 0.02 | 13.30 | 0.02 | 13.23 | 0.04 |
| 40 | 239.63 | 249.19 | 13.98 | 0.03 | 13.28 | 0.02 | 13.27 | 0.07 |
| 41 | 257.79 | 247.60 | 13.98 | 0.03 | 13.29 | 0.02 | 13.26 | 0.05 |
| 42 | 228.29 | 269.11 | 13.97 | 0.03 | 13.30 | 0.02 | 13.27 | 0.04 |

**Table 1.** Continued

| ID | X | Y | $J$ | $\sigma_J$ | $H$ | $\sigma_H$ | $K$ | $\sigma_K$ |
|---|---|---|---|---|---|---|---|---|
| 43 | 297.02 | 337.98 | 14.01 | 0.03 | 13.30 | 0.02 | 13.25 | 0.04 |
| 44 | 51.95 | 196.90 | 14.07 | 0.02 | 13.37 | 0.02 | 13.30 | 0.03 |
| 45 | 390.92 | 34.97 | 13.81 | 0.03 | 13.46 | 0.02 | 13.50 | 0.03 |
| 46 | 317.94 | 465.63 | 13.98 | 0.03 | 13.44 | 0.02 | 13.42 | 0.03 |
| 47 | 420.30 | 271.52 | 13.93 | 0.03 | 13.61 | 0.02 | 13.67 | 0.06 |
| 48 | 134.24 | 331.73 | 14.28 | 0.03 | 13.55 | 0.02 | 13.44 | 0.05 |
| 49 | 187.87 | 104.22 | 14.23 | 0.04 | 13.63 | 0.06 | 13.67 | 0.08 |
| 50 | 112.22 | 211.92 | 14.44 | 0.03 | 13.71 | 0.01 | 13.66 | 0.04 |
| 51 | 239.98 | 359.80 | 14.40 | 0.05 | 13.72 | 0.02 | 13.71 | 0.08 |
| 52 | 148.68 | 208.90 | 14.44 | 0.03 | 13.76 | 0.02 | 13.75 | 0.04 |
| 53 | 251.24 | 120.16 | 14.48 | 0.03 | 13.80 | 0.02 | 13.77 | 0.05 |
| 54 | 171.86 | 269.81 | 14.22 | 0.03 | 13.96 | 0.02 | 13.92 | 0.05 |
| 55 | 58.99 | 325.19 | 14.22 | 0.03 | 14.01 | 0.03 | 13.96 | 0.06 |
| 56 | 211.12 | 305.26 | 14.60 | 0.03 | 13.92 | 0.02 | 13.83 | 0.04 |
| 57 | 152.10 | 265.96 | 15.35 | 0.09 | 13.94 | 0.03 | 13.91 | 0.04 |
| 58 | 216.16 | 348.61 | 14.72 | 0.04 | 14.03 | 0.02 | 13.97 | 0.04 |
| 59 | 343.92 | 287.84 | 14.76 | 0.04 | 14.15 | 0.03 | 13.91 | 0.06 |
| 60 | 241.26 | 460.29 | 14.59 | 0.05 | 14.26 | 0.03 | 14.02 | 0.06 |
| 61 | 85.88 | 188.55 | 14.70 | 0.04 | 14.24 | 0.02 | 14.28 | 0.03 |
| 62 | 411.76 | 27.50 | 14.93 | 0.04 | 14.28 | 0.02 | 14.25 | 0.04 |
| 63 | 221.43 | 270.80 | 15.09 | 0.04 | 14.36 | 0.02 | 14.32 | 0.05 |
| 64 | 439.89 | 106.58 | 15.23 | 0.03 | 14.60 | 0.03 | 14.56 | 0.07 |
| 65 | 113.75 | 275.50 | 15.30 | 0.03 | 14.66 | 0.02 | 14.53 | 0.04 |
| 66 | 36.88 | 250.75 | 15.36 | 0.06 | 14.62 | 0.03 | 14.61 | 0.07 |
| 67 | 277.52 | 34.09 | 15.04 | 0.04 | 14.79 | 0.03 | 14.80 | 0.08 |
| 68 | 103.43 | 16.05 | 15.30 | 0.04 | 14.84 | 0.03 | 14.86 | 0.09 |
| 69 | 226.08 | 359.16 | 15.19 | 0.05 | 14.90 | 0.03 | 14.82 | 0.10 |
| 70 | 278.14 | 201.41 | 15.45 | 0.03 | 14.98 | 0.02 | 15.09 | 0.06 |
| 71 | 303.83 | 287.33 | 15.30 | 0.05 | 15.11 | 0.05 | 15.27 | 0.11 |
| 72 | 381.58 | 445.55 | 15.43 | 0.03 | 15.07 | 0.03 | 15.12 | 0.07 |
| 73 | 189.31 | 238.25 | 15.55 | 0.04 | 14.98 | 0.04 | 15.08 | 0.10 |
| 74 | 319.30 | 95.11 | 15.49 | 0.05 | 15.09 | 0.04 | 15.04 | 0.10 |
| 75 | 215.12 | 334.78 | 15.57 | 0.06 | 15.02 | 0.04 | 15.03 | 0.07 |
| 76 | 182.43 | 243.72 | 15.43 | 0.05 | 15.06 | 0.03 | 15.01 | 0.06 |
| 77 | 367.62 | 181.09 | 15.53 | 0.03 | 15.18 | 0.03 | 15.18 | 0.14 |
| 78 | 375.89 | 241.46 | 15.85 | 0.09 | 15.07 | 0.03 | 15.03 | 0.09 |
| 79 | 66.98 | 477.17 | 15.70 | 0.09 | 15.20 | 0.06 | 14.82 | 0.09 |
| 80 | 81.21 | 97.69 | 15.78 | 0.04 | 15.13 | 0.04 | 14.95 | 0.06 |
| 81 | 286.80 | 332.35 | 15.81 | 0.06 | 15.11 | 0.04 | 15.00 | 0.13 |
| 82 | 55.30 | 225.89 | 15.67 | 0.04 | 15.17 | 0.03 | 15.18 | 0.06 |
| 83 | 190.37 | 180.59 | 15.60 | 0.04 | 15.32 | 0.05 | 15.44 | 0.11 |
| 84 | 64.44 | 311.33 | 15.64 | 0.07 | 15.20 | 0.04 | 15.22 | 0.11 |

**Table 1.** Continued

| ID | X | Y | $J$ | $\sigma_J$ | $H$ | $\sigma_H$ | $K$ | $\sigma_K$ |
|---|---|---|---|---|---|---|---|---|
| 85 | 474.72 | 353.03 | 15.80 | 0.11 | 15.19 | 0.06 | 15.16 | 0.11 |
| 86 | 202.39 | 235.30 | 15.79 | 0.05 | 15.23 | 0.04 | 15.25 | 0.10 |
| 87 | 431.66 | 401.00 | 15.79 | 0.06 | 15.24 | 0.05 | 15.28 | 0.11 |
| 88 | 180.15 | 49.52 | 16.05 | 0.07 | 15.18 | 0.09 | 15.01 | 0.10 |
| 89 | 204.76 | 265.27 | 15.67 | 0.06 | 15.36 | 0.04 | 15.16 | 0.05 |
| 90 | 125.40 | 119.06 | 15.73 | 0.04 | 15.44 | 0.05 | 15.20 | 0.10 |
| 91 | 442.82 | 39.01 | 15.71 | 0.06 | 15.34 | 0.04 | 15.35 | 0.12 |
| 92 | 24.86 | 393.23 | 15.72 | 0.08 | 15.30 | 0.03 | 15.34 | 0.15 |
| 93 | 344.03 | 347.37 | 15.77 | 0.06 | 15.19 | 0.05 | 15.33 | 0.04 |
| 94 | 163.57 | 160.30 | 15.83 | 0.04 | 15.35 | 0.05 | 15.24 | 0.05 |
| 95 | 232.06 | 362.59 | 15.68 | 0.09 | 15.36 | 0.08 | 15.39 | 0.12 |
| 96 | 319.91 | 437.30 | 15.97 | 0.07 | 15.28 | 0.05 | 15.25 | 0.12 |
| 97 | 333.24 | 142.52 | 15.71 | 0.07 | 15.33 | 0.04 | 15.52 | 0.14 |
| 98 | 56.32 | 293.02 | 15.55 | 0.06 | 15.50 | 0.06 | 15.52 | 0.07 |
| 99 | 159.40 | 227.32 | 15.95 | 0.10 | 15.40 | 0.05 | 15.30 | 0.05 |
| 100 | 195.45 | 286.60 | 15.79 | 0.06 | 15.46 | 0.03 | 15.38 | 0.08 |
| 101 | 244.55 | 199.77 | 15.85 | 0.04 | 15.69 | 0.05 | 15.45 | 0.06 |
| 102 | 258.72 | 240.88 | 15.93 | 0.05 | 15.64 | 0.06 | 15.47 | 0.19 |
| 103 | 102.45 | 190.01 | 15.82 | 0.04 | 15.47 | 0.02 | 15.48 | 0.08 |
| 104 | 3.84 | 350.33 | 16.03 | 0.09 | 15.44 | 0.05 | 15.40 | 0.18 |
| 105 | 225.56 | 276.05 | 15.89 | 0.07 | 15.46 | 0.03 | 15.45 | 0.06 |
| 106 | 286.72 | 133.40 | 15.93 | 0.09 | 15.59 | 0.05 | 15.49 | 0.14 |
| 107 | 12.33 | 204.49 | 16.09 | 0.06 | 15.58 | 0.06 | 15.50 | 0.09 |
| 108 | 251.58 | 384.73 | 15.91 | 0.07 | 15.63 | 0.04 | 15.61 | 0.13 |
| 109 | 157.26 | 10.90 | 16.10 | 0.09 | 15.55 | 0.07 | 15.73 | 0.18 |
| 110 | 234.55 | 283.18 | 15.92 | 0.08 | 15.57 | 0.03 | 15.67 | 0.11 |
| 111 | 186.58 | 136.20 | 16.01 | 0.14 | 15.55 | 0.12 | 15.84 | 0.22 |
| 112 | 259.22 | 32.14 | 15.96 | 0.04 | 15.68 | 0.03 | 15.69 | 0.08 |
| 113 | 333.45 | 303.44 | 16.02 | 0.07 | 15.69 | 0.06 | 15.52 | 0.11 |
| 114 | 153.52 | 301.36 | 15.94 | 0.09 | 15.60 | 0.08 | 16.01 | 0.17 |
| 115 | 136.07 | 210.46 | 16.24 | 0.17 | 15.52 | 0.08 | 15.56 | 0.08 |
| 116 | 160.96 | 223.02 | 16.00 | 0.05 | 15.79 | 0.06 | 15.89 | 0.14 |
| 117 | 228.35 | 73.24 | 16.23 | 0.06 | 15.66 | 0.04 | 15.52 | 0.06 |
| 118 | 315.08 | 211.17 | 16.03 | 0.05 | 15.77 | 0.06 | 15.84 | 0.09 |
| 119 | 209.63 | 116.20 | 15.96 | 0.04 | 15.85 | 0.04 | 15.79 | 0.07 |
| 120 | 324.01 | 330.53 | 16.13 | 0.08 | 15.70 | 0.06 | 15.74 | 0.09 |
| 121 | 113.21 | 200.78 | 16.02 | 0.05 | 15.84 | 0.04 | 15.77 | 0.08 |
| 122 | 268.76 | 43.58 | 16.14 | 0.05 | 15.81 | 0.05 | 16.03 | 0.25 |
| 123 | 154.83 | 316.02 | 16.13 | 0.08 | 15.70 | 0.04 | 15.84 | 0.09 |
| 124 | 26.99 | 453.36 | 15.99 | 0.09 | 15.72 | 0.04 | 15.73 | 0.06 |
| 125 | 258.43 | 227.84 | 16.16 | 0.04 | 15.85 | 0.05 | 15.91 | 0.10 |
| 126 | 287.97 | 249.77 | 16.15 | 0.14 | 15.83 | 0.19 | 15.71 | 0.11 |
| 127 | 317.30 | 365.52 | 16.15 | 0.06 | 15.92 | 0.07 | 15.82 | 0.17 |

**Table 1.** Continued

| ID | X | Y | $J$ | $\sigma_J$ | $H$ | $\sigma_H$ | $K$ | $\sigma_K$ |
|---|---|---|---|---|---|---|---|---|
| 128 | 251.13 | 158.73 | 16.18 | 0.04 | 15.97 | 0.07 | 15.96 | 0.10 |
| 129 | 13.49 | 83.62 | 16.58 | 0.15 | 15.67 | 0.04 | 15.72 | 0.06 |
| 130 | 289.57 | 289.86 | 16.38 | 0.14 | 15.74 | 0.07 | 15.67 | 0.19 |
| 131 | 246.47 | 31.71 | 16.54 | 0.12 | 15.72 | 0.05 | 15.71 | 0.17 |
| 132 | 156.40 | 305.40 | 16.11 | 0.10 | 15.90 | 0.09 | 15.94 | 0.19 |
| 133 | 232.28 | 163.17 | 16.23 | 0.10 | 15.77 | 0.03 | 15.79 | 0.08 |
| 134 | 132.90 | 243.32 | 16.25 | 0.08 | 15.84 | 0.04 | 15.52 | 0.13 |
| 135 | 171.21 | 382.43 | 16.09 | 0.10 | 15.88 | 0.06 | 15.92 | 0.16 |
| 136 | 120.03 | 279.01 | 16.20 | 0.08 | 15.86 | 0.06 | 16.17 | 0.19 |
| 137 | 249.45 | 184.07 | 16.11 | 0.08 | 15.98 | 0.07 | 15.92 | 0.11 |
| 138 | 183.65 | 156.01 | 16.39 | 0.06 | 16.15 | 0.10 | 15.77 | 0.18 |
| 139 | 467.39 | 28.85 | 16.31 | 0.07 | 15.92 | 0.06 | 15.87 | 0.08 |
| 140 | 262.94 | 249.81 | 16.57 | 0.07 | 15.81 | 0.06 | 15.85 | 0.10 |
| 141 | 253.04 | 265.83 | 16.29 | 0.09 | 15.94 | 0.05 | 15.78 | 0.18 |
| 142 | 133.18 | 279.96 | 16.41 | 0.06 | 16.14 | 0.09 | 15.88 | 0.17 |
| 143 | 247.77 | 204.53 | 16.32 | 0.05 | 15.97 | 0.03 | 15.84 | 0.19 |
| 144 | 134.32 | 114.54 | 16.39 | 0.11 | 16.00 | 0.09 | 15.90 | 0.13 |
| 145 | 117.18 | 201.28 | 16.32 | 0.08 | 16.01 | 0.06 | 16.05 | 0.16 |
| 146 | 86.49 | 135.81 | 16.42 | 0.12 | 15.99 | 0.06 | 15.77 | 0.08 |
| 147 | 208.16 | 235.83 | 16.24 | 0.07 | 16.09 | 0.06 | 16.24 | 0.15 |
| 148 | 259.00 | 356.29 | 16.43 | 0.05 | 16.11 | 0.09 | 15.97 | 0.08 |
| 149 | 177.73 | 292.41 | 16.18 | 0.11 | 16.00 | 0.06 | 16.26 | 0.18 |
| 150 | 181.04 | 251.70 | 16.44 | 0.12 | 15.95 | 0.05 | 15.88 | 0.06 |
| 151 | 158.35 | 249.59 | 16.31 | 0.12 | 16.08 | 0.11 | 15.93 | 0.10 |
| 152 | 75.94 | 198.40 | 16.56 | 0.17 | 15.87 | 0.06 | 16.04 | 0.10 |
| 153 | 126.84 | 183.29 | 16.30 | 0.06 | 16.02 | 0.04 | 16.01 | 0.08 |
| 154 | 96.67 | 344.14 | 16.35 | 0.09 | 15.94 | 0.04 | 16.07 | 0.08 |
| 155 | 309.61 | 178.91 | 16.33 | 0.08 | 16.17 | 0.07 | 15.85 | 0.13 |
| 156 | 255.06 | 55.91 | 16.25 | 0.11 | 15.96 | 0.04 | 16.07 | 0.10 |
| 157 | 238.60 | 255.98 | 16.38 | 0.10 | 15.98 | 0.05 | 16.41 | 0.31 |
| 158 | 302.13 | 456.82 | 16.42 | 0.06 | 16.05 | 0.05 | 15.91 | 0.09 |
| 159 | 47.37 | 403.21 | 16.55 | 0.13 | 16.01 | 0.06 | 15.82 | 0.08 |
| 160 | 244.27 | 274.91 | 16.64 | 0.06 | 15.96 | 0.05 | 15.87 | 0.08 |
| 161 | 166.90 | 208.20 | 16.49 | 0.12 | 15.96 | 0.05 | 16.13 | 0.20 |
| 162 | 159.33 | 350.71 | 16.26 | 0.11 | 16.10 | 0.06 | 15.89 | 0.13 |

band. Although this cluster is faint, the data reached fairly deep down to $V\sim21$ mag. Phelps et al. (1994) published $U-B$ CCD data for bright stars in this cluster. In order to minimize the contamination of field stars, we determined the major contribution radius of To 2 member stars as 160" from Kubiak et al. (1994)'s Fig. 1. Following analysis uses those stars whose distance from the cluster center is less than $R\sim160$".

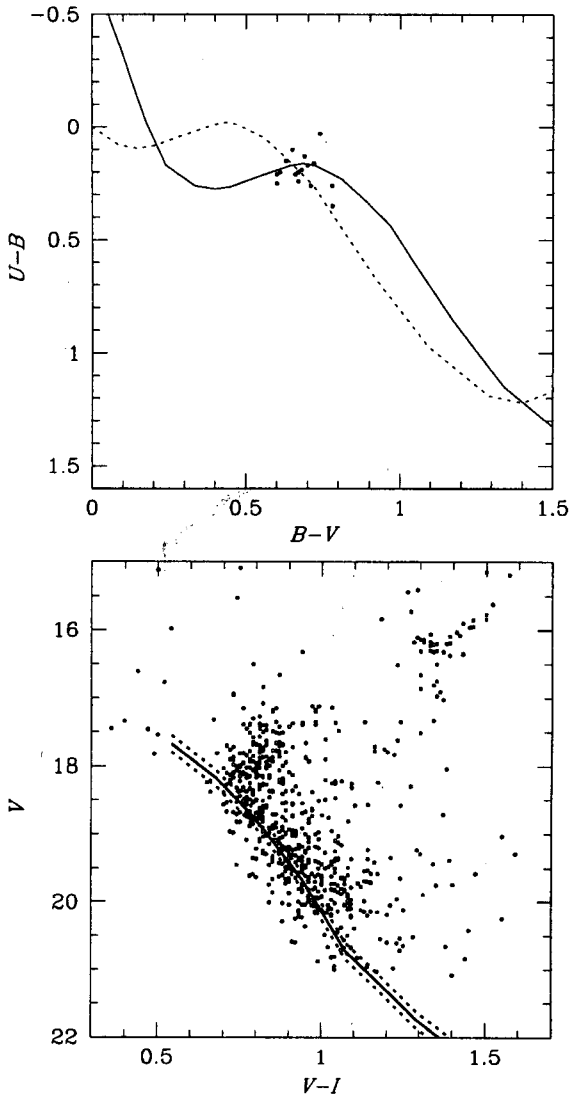


**Fig. 3.** ($U-B$, $B-V$) diagram of To 2 (*above*). The solid line and dashed line represent the ZAMS given by Sung & Bessell (1999), reddened according to $E(B-V)=0.23$. The star used in the fitting are located in the main sequence turn-off point in ($V$, $B-V$) CMD and inside the radius R<160". ZAMS fitting to ($V$, $V-I$) CMD (*below*). Solid line represents the ZAMS line, shifted according to the reddening and distance of To 2. The dashed line represents the fitting error of the distance modulus.

### (a) Reddening and Distance Modulus

The prevailing method of determining the reddening value traditionally is using the two color diagram. With Sung & Bessell (1999) ZAMS data, we determined the reddening value of To 2 as $E(B-V)=0.23\pm0.03$, as shown in Fig. 3. Although the $U$ band data observed by Phelps et al. (1994) is insufficient, the data exist near the main sequence turn-off point in ($V$, $B-V$) CMD. Excluding several data deviated from the turn-off point, we used all data in this fitting.

Another method is using the mean magnitude and color of red giant clump stars (RGC). Janes & Phelps (1994) derived $M_V=0.90\pm0.40$ and $(B-V)_0=0.95\pm0.12$ for the clumps of open clusters with $\delta V$ (their age parameter) >1.0. The RGC mean color of To 2 is determined as $(B-V)=1.20\pm0.03$. From this, we determined $E(B-V)=0.25\pm0.12$. The two values derived from two widely different methods are very compatible. Our best estimate for reddening is therefore $E(B-V)=0.24\pm0.12$.

The distance modulus can be determined using either ZAMS fitting or the mean magnitude of RGC stars. Since the ($B-V$) color is affected by metal deficiency (Sung & Bessell, 1999), we use ($V$, $V-I$) CMD obtained by Phelps et al. (1994) to derive the distance modulus. With the above determined value of $E(B-V)=0.24$, ZAMS fitting shows $(m-M)_V=15.2\pm0.12$ as seen in Fig. 3 (*below*). The mean magnitude of RGC stars, on the other hand, is $V_{RGC}=16.16\pm0.12$. The distance modulus implied is $(m-M)_V=15.3\pm0.42$, which is identical to the other estimate. Adopting $A_V=3.2$ $E(B-V)$, we derive $(m-M)_0=14.6\pm0.42$. Friel & Janes (1993) determined reddening and distance modulus as 0.20, 15.3, respectively. Kubiak et al. (1992) estimated $E(B-V)=0.40$, $(m-M)_0=14.0$ from a direct comparison of their C-M diagram with theoretical isochrones. But these values are considerably higher than those derived by us and Friel & Janes (1993). It appears that Kubiak et al. (1992) overestimated the reddening value, which resulted in the underestimated distance modulus.

### (b) Age and Metallicity

The metallicity estimate of star cluster can be made from the ultraviolet excess in the ($U-B$, $B-V$) diagram (Sandage 1969). But the available $U$ band data of To 2 is not enough to estimate the metallicity using this two color diagram method. Therefore, we chose an isochrone approach which make use of theoretical calculations of stellar evolution for various cases of age and metallicity. By assuming the reddening and distance modulus obtained in previous section, we fit theoretical isochrones to the $BV$ $C$-$M$ diagrams (Kubiak et al., 1992), and then attempted to estimate age and metallicity simultaneously. The Bertelli et al. (1994) models are

**Table 2.** Basic Parameters of To 2

| Parameter | This Study | Previous Studies |
|---|---|---|
| $E(B-V)$ | 0.24 | 0.08[1], 0.1[2], 0.4[3], 0.3-0.4[4], 0.2[5] |
| $(m-M)_0$ | 14.6 | 14.0[3] |
| Metallicity | −0.3 | −1.2[2] −0.3[4] −0.6[5] |
| log $t$ | 9.3 | 8.9[1] 9.6[3] 9.4[6] |

1. Adler & Janes (1982), photographic; 2. Geisler (1987), Washington photoelectric; 3. Kubiak et al. (1992), CCD; 4. Brown et al. (1996), spectroscopic; 5. Friel & Janes (1993), spectroscopic; 6. Phelps et al. (1994), CCD

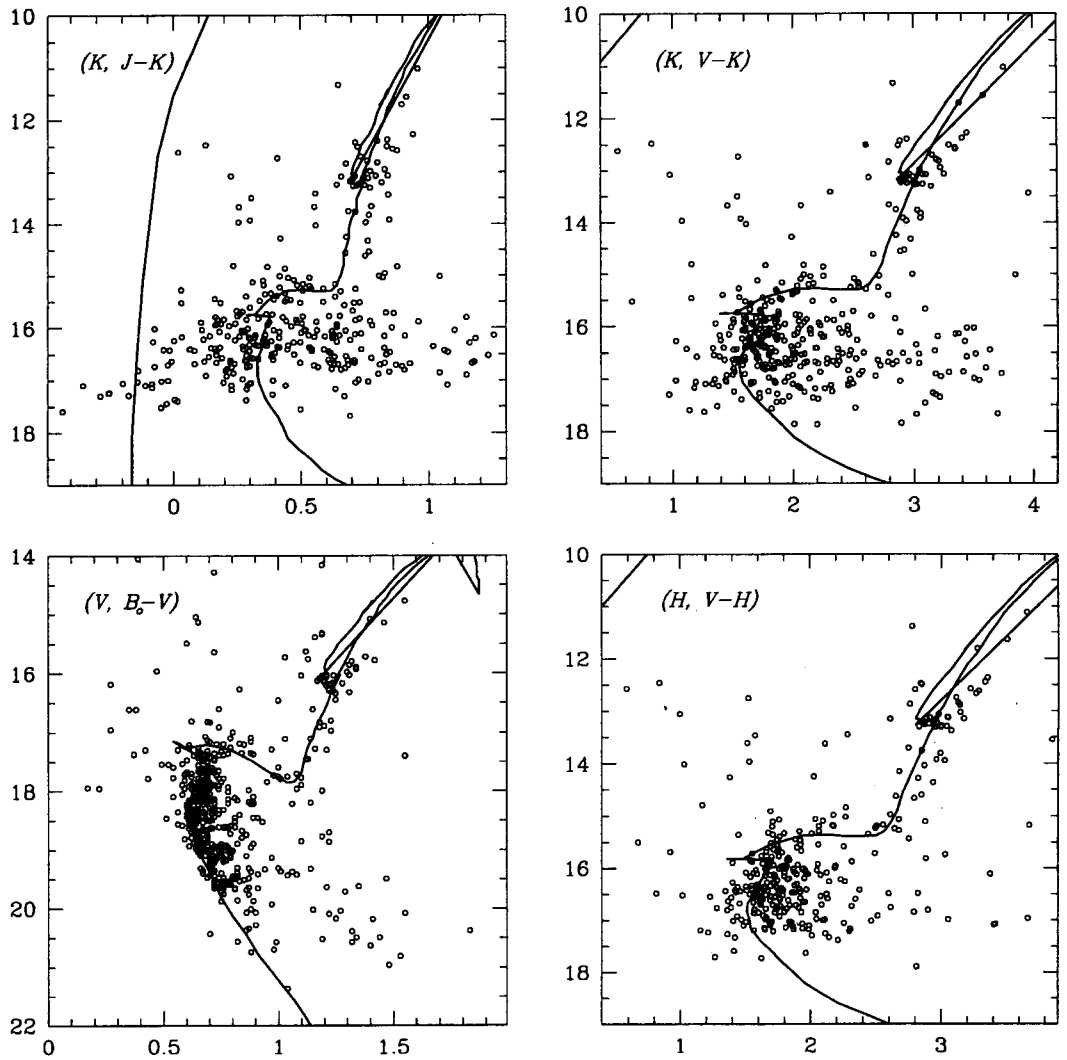


**Fig. 4.** The isochrone with log $t$=9.3, [Fe/H]=−0.32, $E(B-V)$=0.24, $(m-M)_0$=14.6 over-imposed to our IR CMD. Only the stars detected in both optical and IR band are presented.

compared to observed CMDs because several studies give preference toward models with convective overshooting (Carraro et al. 1993, 1994). The considered age and metallicity ranged from log $t$=9.1 to 9.5 and [Fe/H]=−1.0 to +0.47. Isochrones were shifted in color and magnitude space with the adopted $E(B-V)$ and $(m-M)_O$.

Most isochrones were readily discarded as possible candidates because they poorly matched the turnoff region and the slope of the main sequence. Acceptability was based on how well the isochrones described the turnoff, main sequence line and the location of the red giant clump. From the entire grid of isochrones, we determined the best matched one as isochrone with log $t$=9.3 and [Fe/H]=−0.32. Our metallicity, derived this way, is very different with Geisler (1987)'s value. We note that Geisler used bright stars, $V$~6 to 9, for his Washington photometry. These stars were probably field stars rather than true members of To 2, as its giant stars are located around $V$~16.

Finally the best matched isochrone is over-imposed on multi-color CMD in Fig. 4 in order to verify that the derived basic parameters are compatible for near-infrared domain as well. We used a total of 530 stars, for which both optical and near-infrared data are available. The adopted reddening relations are from Bessell & Brett (1988). That is, $E(V-K)=2.74E(B-V)$, $E(J-K)=0.52\ E(B-V)$, $E(V-H)=2.68E(B-V)$. As seen in the figure, the theoretical isochrones demonstrate that our basic parameters give good matches to the main sequence region of CMDs which cover entire spectrum domain from $B$ to $K$ passbands. Nevertheless, the subgiant branch, giant branch and clump data are redder than the theoretical prediction in optical band. Such gap is more evident in IR band.

## V. SUMMARY

We presented near-IR ($JHK$ band) photometric data of

the distant old open cluster To 2. The characteristics such as reddening, distance modulus, age and metallicity were derived using the published optical data (Kubiak et al., 1992) and updated theoretical isochrones (Bertelli et al., 1994). We include $E(B-V)=0.24\pm0.12$ by using two-color diagram and mean color of red giant clump star, $(m-M)_0=14.6\pm0.42$ by using ZAMS fitting and mean magnitude of RGC stars, and log $t\sim9.3$ and [Fe/H]$\sim-0.3$ using isochrone fitting method. The deriv-ed parameters and theoretical isochrones based on them are found to explain major CMD features across a very wide wavelength range from $B$ to $K$ passband.

Because of its location in the outer disk, To 2 is an important cluster in understanding the chemical gradient and formation mechanism for galactic disk. However, previous studies showed widely different estimates for basic parameters such as distance, age and metallicity. Our estimates provide more reliable constraints to these parameters as demonstrated by isochrone-CMD comparisons. Our results are compared with previous studies in Table 2.

We would like to thank the support staffs at Siding Spring Observatory for their assistance during our observing run. We also thank Dr. Kubiak who supplied his optical data to be used in our analysis. This work was supported by Star Project and Large Telescope project funded by Korea Minitry of Science and Technology and Korea Astronomy Observatory. YIB acknowledges the support of KOSEF Grant No. 2000- 113-03-2.

## REFERENCES

Adler, D. S. & Janes, K. A. 1982, PASP, 94, 905
Bertelli, G., Bressan, A., Chiosi, C., Fagotto, F. & Nasi, E. 1994 A&AS, 106, 275
Bessell, M. S. & Brett, J. M. 1988, PASP, 100, 1134
Brown, J. A., Wallerstein, G., Geisler, D. & Oke, J. B. 1993, AJ, 112, 1551
Carraro, G., Bertelli, G., Bressan, A. & Chiosi, C. 1993, A&AS, 101, 381
Carraro, G., Chiosi, C., Bressan, A. & Bertelli, G. 1994, A&AS, 103, 375
Friel, E. D. 1995, ARAA, 33, space 381
Friel, E. D. & Janes, K. A. 1993, A&A, 267, 75
Friel, E. D., Janes, K. A., Hong, L., Lotz, J. & Tavarez, M. 1995, The formation of the Milky way eds. by E. J. Alfaro & G. Tenero-Tagle (Cambridge Univ.: Cambridge), 189
Geisler, D. 1987, AJ, 94, 84
Janes, K. A. & Phelps, R. L. 1994, AJ, 108, 1773
Kubiak, M., Kaluzny, J., Krzeminski, W. & Mateo, M. 1992, Acta Astronomica, 42, 155
McGregor, P. 1995, *Users Manual for the CASPIR on the MSSSO 2.3m Telescope*
Phelps, R. L., Janes, K. A. & Montgomery, K. A. 1994, AJ, 107, 1079
Sandage, A. 1969, ApJ, 158, 1115
Stetson, P. B. 1992, IAU Colloq. 136, *Stellar Photometry, Current Techniques and Future Development*, eds by C. J. Butler & I. Elliot(Cambridge Univ. Press:Cambridge), 291
Sung, H. & Bessell, M. S. 1999, MNRAS, 306, 36